The Astrophysical Journal, 793:35 (10pp), 2014 September 20 doi:10.1088/0004-637X/793/1/35

THE LONGITUDINAL DEPENDENCE OF HEAVY-ION COMPOSITION IN THE 2013 APRIL 11 SOLAR ENERGETIC PARTICLE EVENT

C. M. S. Cohen[1], G. M. Mason[2], R. A. Mewaldt[1], and M. E. Wiedenbeck[3]
[1] California Institute of Technology, Pasadena, CA 91125, USA
[2] Applied Physics Laboratory, Johns Hopkins University, Laurel, MD 20723, USA
[3] Jet Propulsion Laboratory, California Institute of Technology, Pasadena, CA 91109, USA
Received 2014 February 27; accepted 2014 July 16; published 2014 September 3

ABSTRACT

On 2013 April 11 active region 11719 was centered just west of the central meridian; at 06:55 UT, it erupted with an M6.5 X-ray flare and a moderately fast (∼800 km s^{-1}) coronal mass ejection. This solar activity resulted in the acceleration of energetic ions to produce a solar energetic particle (SEP) event that was subsequently observed in energetic protons by both *ACE* and the two *STEREO* spacecraft. Heavy ions at energies ⩾10 MeV $nucleon^{-1}$ were well measured by SEP sensors on *ACE* and *STEREO-B*, allowing the longitudinal dependence of the event composition to be studied. Both spacecraft observed significant enhancements in the Fe/O ratio at 12–33 MeV $nucleon^{-1}$, with the *STEREO-B* abundance ratio (Fe/O = 0.69) being similar to that of the large, Fe-rich SEP events observed in solar cycle 23. The footpoint of the magnetic field line connected to the *ACE* spacecraft was longitudinally farther from the flare site (77° versus 58°), and the measured Fe/O ratio at *ACE* was 0.48, 44% lower than at *STEREO-B* but still enhanced by more than a factor of 3.5 over average SEP abundances. Only upper limits were obtained for the ^{3}He/^{4}He abundance ratio at both spacecraft. Low upper limits of 0.07% and 1% were obtained from the *ACE* sensors at 0.5–2 and 6.5–11.3 MeV $nucleon^{-1}$, respectively, whereas the *STEREO-B* sensor provided an upper limit of 4%. These characteristics of high, but longitudinally variable, Fe/O ratios and low ^{3}He/^{4}He ratios are not expected from either the direct flare contribution scenario or the remnant flare suprathermal material theory put forth to explain the Fe-rich SEP events of cycle 23.

Key words: acceleration of particles – Sun: activity – Sun: coronal mass ejections (CMEs) – Sun: particle emission

Online-only material: color figures

1. INTRODUCTION

One of the surprising results from the studies of solar energetic particle (SEP) events of solar cycle 23 was the recognition of large, Fe-rich SEP events (Cohen et al. 1999a,1999b; Mason et al. 1999). In the two-class paradigm language of Reames (1999), these were "gradual" SEP events in that they lasted for days, were associated with wide, fast coronal mass ejections (CMEs) driving a shock, and exhibited type II radio bursts. However, they also had a composition that was more typical of "impulsive" (i.e., flare-related) events with high Fe/O ratios and enhanced ^{3}He/^{4}He ratios (although not reaching the very high values typically observed in impulsive events). Most of these cycle 23 events (referred to here as Fe-rich SEP events) were observed during the rising phase of the cycle and typically had hard power-law ion spectra and enhanced Fe/O across a wide range of energies. This is illustrated in Figure 1 for five Fe-rich events observed by instruments on *ACE* from 1997 to 1998. For all the events, the oxygen spectra are harder than E^{-3} (left panel) and, across a wide range of energies, the Fe/O ratio is significantly higher than the average gradual SEP event value of 0.134 determined by Reames (1998) at 5–12 MeV $nucleon^{-1}$ (henceforth referred to as the average Fe/O value; right panel). With the exception of 1998 May 2, all these events had ^{3}He/^{4}He abundance ratios enhanced by factors of ∼10–100 (at 8–14 MeV $nucleon^{-1}$) over the solar wind value, which was assumed to be typical of gradual SEP events. Occasionally, Fe-rich SEP events have exhibited an increase in the Fe/O ratio with increasing energy such that the Fe/O enhancement is most apparent at energies >10 MeV $nucleon^{-1}$ (e.g., Tylka et al. 2005).

Several scenarios were put forth to explain the creation of these events. The direct flare contribution idea (Cane et al. 2003, 2006) assumes that particles are being accelerated both by the associated flare and the CME-driven shock, and that the Fe-rich material is accelerated directly by flare-related processes in the same manner as in smaller, impulsive events. Whether or not this material is observed depends on how well an observer is magnetically connected to the flaring region, what energy is being measured, and how strong the shock is. For well-connected observers, Cane et al. (2003) concluded that the flare-accelerated material would be evident at energies above that typical for the shock-accelerated material (∼20 MeV $nucleon^{-1}$). For measurements made at locations far removed from the field line connected to the solar source, only shock-accelerated material would be observed. This would result in a longitudinal dependence to the Fe/O ratios with higher values observed at longitudes more closely connected magnetically to the flaring region. Additionally, an energy dependence to the Fe/O ratio (with increasing Fe/O ratios with increasing energy) would be observed at locations magnetically well connected to the solar source.

The remnant flare suprathermal material scenario assumes that all the observed SEPs are accelerated by the CME-driven shock (Tylka et al. 2005; Tylka & Lee 2006; see also Mason et al. 1999). Specific to the Tylka et al. (2005) model, whether the population is enhanced in Fe depends on the orientation of the shock, as well as the availability of a suprathermal population created by a previous flaring activity (i.e., remnant flare material). The concept relies on the idea that quasi-perpendicular shocks have a higher injection energy threshold and the remnant flare material will have a harder spectrum

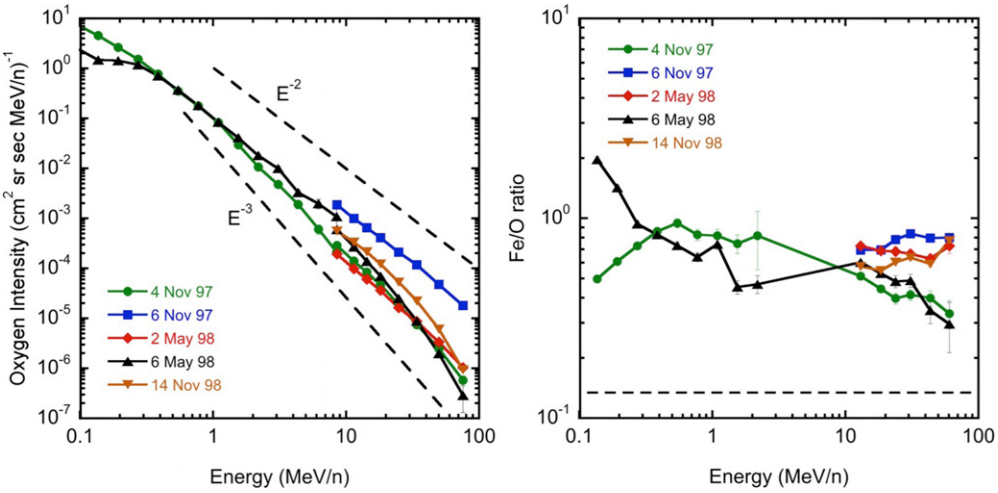

Figure 1. Left: oxygen energy spectra for five Fe-rich events observed in solar cycle 23. Lines corresponding to power-law spectra with indices of two and three are shown for reference. Right: Fe/O abundance ratios as a function of energy for the same five events. The higher energy data are from *ACE*/SIS; the lower energy data are from *ACE*/ULEIS (shown for only two events as during the other events ULEIS suffered significant loss in efficiency due to saturation effects). The dashed line indicates the average Fe/O value as determined by Reames (1998) for gradual SEP events.

(A color version of this figure is available in the online journal.)

than the solar wind suprathermals, which together create a seed particle population that has an energy-dependent Fe/O abundance. A quasi-perpendicular shock will accelerate more flare suprathermals, whereas a quasi-parallel shock, with its lower injection energy threshold, will accelerate mostly solar wind suprathermal particles. Thus, an Fe-rich SEP event will be observed when a quasi-perpendicular shock accelerates remnant flare suprathermal particles. As the seed population already has an energy dependence to the Fe/O ratio, and quasi-perpendicular shocks more effectively accelerate particles to higher energies, the resulting SEP event will have an increasing Fe/O ratio with increasing energy. Although, in general, there is no expected longitudinal dependence to the Fe/O ratio in this scenario, one could potentially result from the fact that quasi-perpendicular shocks may be more likely to occur on the flanks of the shock created by the expanding CME. In that case, any resulting longitudinal dependence would be significantly different than that expected from the direct flare contribution scenario.

Another concept, which is almost a hybrid of the previous two, involves the reacceleration of flare-accelerated SEPs (Li et al. 2005). Here, particles accelerated by flare-related processes stream out of the region ahead of the CME-driven shock, and may be scattered and return to the shock as it moves outward from the Sun and thus be further accelerated. Observers will see a combination of flare-accelerated material, flare material reaccelerated by the shock, and shock-accelerated non-flare material, with the first two having enhanced Fe/O ratios. The observed Fe/O abundance will depend on the observer's position and the strength of the shock. Although it is expected that most SEPs will be accelerated by the shock, there will be a longitudinal dependence to the Fe/O ratio, with higher values apparent for observers more directly connected to the flare location, which is similar to that of the direct flare contribution concept.

Testing these ideas requires not only abundance measurements made over a wide range of energies, but also, ideally, similar measurements made simultaneously at different longitudinal locations during an SEP event. This capability became available in 2006 with the launch of the twin *STEREO* spacecraft. Although the large SEP event of 2006 December 13 was Fe-rich and observed by *ACE* and one of the two *STEREO*s (Cohen et al. 2008), there was no significant difference in longitude between the spacecraft to provide insight on the longitudinal dependence of the SEP composition. Unfortunately, the ensuing solar minimum was long and no SEP events of significant size were observed until mid-2010. The longitudinal dependences of H/He and Fe/O ratios were studied for 22 relatively small events occurring between 2009 January and 2011 February using data from instrumentation on *ACE* and *STEREO* at energies <1 MeV nucleon^{-1} (Cohen et al. 2012), however, these energies were significantly lower than ideal for testing the scenarios described previously. As larger multi-spacecraft events occurred in 2011 and 2012, it became possible to study the composition at energies $\geqslant 10$ MeV nucleon^{-1} for 12 large SEP events (Cohen et al. 2013). Although no systematic dependence was observed in the Fe/O ratios, it was noted that only three of the 12 events had Fe/O ratios more than twice that of the average Fe/O value.

Prior to 2013, no large SEP events exhibited substantial (e.g., $>3\times$ average) enhancements of Fe/O at energies $\geqslant 10$ MeV nucleon^{-1} during solar cycle 24. This is in stark contrast to cycle 23, in which most of the Fe-rich SEP events were observed during the rising phase. In fact, 4 of the first 9 events observed in heavy ions above 10 MeV nucleon^{-1} had Fe/O values >0.7 (Cohen et al. 1999b) and 9 of 12 were Fe-rich (i.e., $>2\times$ average) at 25–80 MeV nucleon^{-1} (Cane et al. 2006). On 2013 April 11, a large SEP event was observed by *ACE* and the *STEREO* spacecraft. The intensities of heavy ions at energies exceeding 10 MeV nucleon^{-1} were examined and the event was found to be Fe-rich. In the following sections we detail the characteristics of this event and discuss the implications of the observed longitudinal dependences for the scenarios put forth to explain the Fe-rich events of cycle 23.

2. OBSERVATIONS

The SEP data presented here were obtained by the Ultra-Low-Energy Isotope Spectrometer (ULEIS; Mason et al. 1998) and the Solar Isotope Spectrometer (SIS; Stone et al. 1998) on *ACE*, and the Suprathermal Ion Telescope (SIT; Mason et al. 2008) and the Low-Energy Telescope (LET; Mewaldt et al.

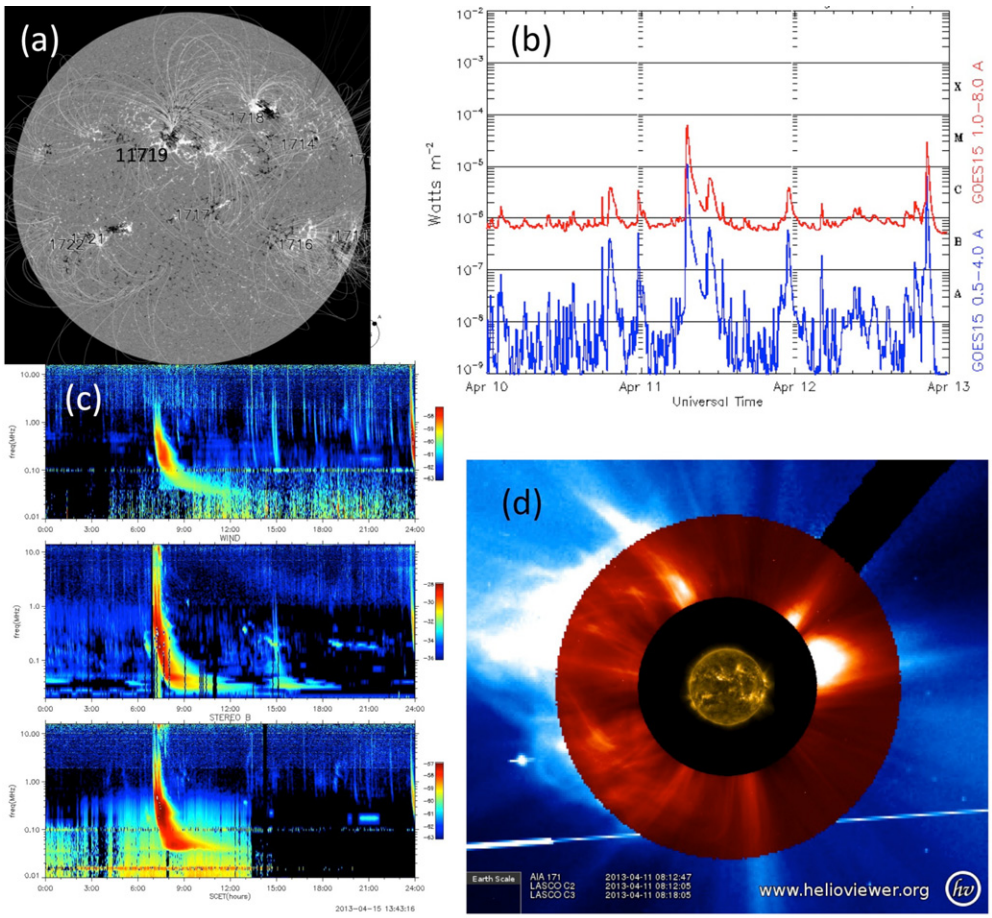

Figure 2. (a) Magnetogram of the solar disk showing the active region 11719 (*Solar Dynamics Observatory* (*SDO*)/Helioseismic and Magnetic Imager image from solarmonitor.org). (b) Time profiles of soft X-rays; the associated X-ray event is an M6.5 at 7:16 on 2013 April 11 (*GOES* plot from swpc.noaa.gov). (c) Radio burst observations for April 11 (*Wind*+*STEREO* plot from swaves.gsfc.nasa.gov). (d) The associated coronal mass ejection as observed by LASCO/C2 and LASCO/C3; the CME is the bright eruption on the left side of the image (solar disk image is from *SDO*/Atmospheric Imaging Assembly; composite image from helioviewer.org). (A color version of this figure is available in the online journal.)

2008) on the *STEREO* spacecraft. The combined SIT + LET data provide measurements of SEPs with element and energy coverage similar to that of ULEIS + SIS. Observations made during the 2006 December events and the first few months of 2007, when the *STEREO* spacecraft were in close proximity to *ACE*, allowed cross-calibrations to be made between the sensors, making it possible to compare SIT/LET and ULEIS/SIS measurements with confidence.

On 2013 April 11, active region 11719, centered at N10W01 (Figure 2(a)), erupted with an M6.5 X-ray flare at 06:55 UT (at N07E13). The soft X-ray emission peaked at 07:16 as shown in Figure 2(b) and type III and II radio bursts (signatures of escaping energetic electrons and the presence of a coronal shock, respectively) were observed at *STEREO* and *Wind* (Figure 2(c)). A CME was observed by the SECCHI coronagraphs on both *STEREO*s and the Large Angle and Spectrometric Coronagraph (LASCO) on *Solar and Heliospheric Observatory* at 07:54 and 07:24, respectively. The observations indicate that the CME was moderately fast (between ∼570 and 860 km s^{-1}, depending on the analysis and observing spacecraft) and wide (between 150° and 360°); the composite view from LASCO C2 + C3 is shown in Figure 2(d). This event occurred during a relatively quiet time period, with no CMEs with widths >60° and speeds >400 km s^{-1} observed during the preceding six days. There were six other flaring active regions on the Earth-observable solar disk, producing 22 C-class flares (with the largest being C4.2), but no M- or X-class flares, for the previous four days.

The SEP event was observed by *ACE* as well as *STEREO-B*, which was at −142° longitude relative to the Sun–Earth line. *STEREO-A*, at 133°, only observed a slight increase in the >25 MeV proton intensity (Richardson et al. 2014) and will not be discussed further in this paper. The relative positions of the three spacecraft and the source region are illustrated in Figure 3. Figure 4 shows the time profiles of He at several energies from *STEREO-B* and *ACE*. In spite of the flaring region being well over the limb as viewed by *STEREO-B*, the rise of the He intensities is fairly quick and not dissimilar to that seen at *ACE*. The prompt peak and exponential decay seen by *STEREO-B* is typical of SEP events with western source regions, whereas the slight plateau leading to a peak at the shock passage in the 0.5 MeV nucleon^{-1} intensities observed by *ACE* is roughly as expected from an event originating near central meridian (see, e.g., Cane et al. 1988). The fact that this behavior is not evident in the 4 MeV nucleon^{-1} *ACE* intensities suggests that the shock was not particularly strong when it reached 1 AU. Not surprisingly, given its distant longitudinal position relative to the source region, *STEREO-B* did not observe an interplanetary shock. Figure 5 contains the time profiles for 1.1 MeV nucleon^{-1} He, O, and Fe for the two spacecraft; here it is already apparent that the composition is not quite the same

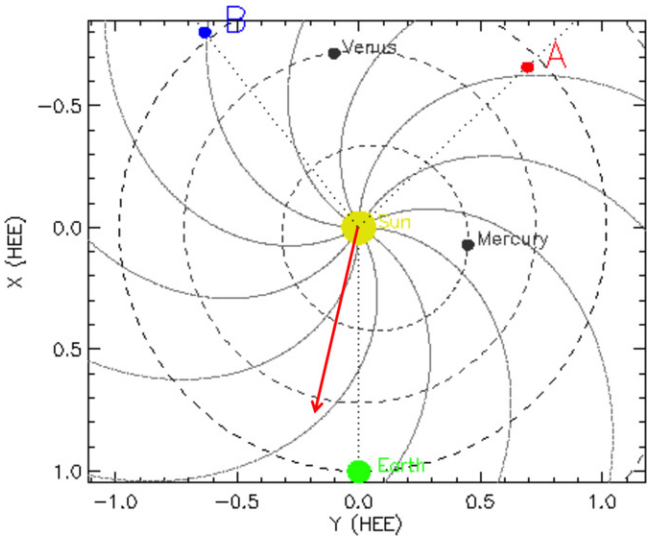

Figure 3. Relative positions of *ACE* (green dot), *STEREO-B* (blue dot), and *STEREO-A* (red dot) at the time of the 2013 April 11 event. The red arrow indicates the longitudinal position of the flare. Nominal Parker spiral field lines are also indicated (adapted from http://stereo-ssc.nascom.nasa.gov/where.shtml).

(A color version of this figure is available in the online journal.)

at the two spacecraft, although both exhibit enhanced Fe/O. On *STEREO-B* the Fe trace is nearly on top of that of O, while the two are more separated in the *ACE* data, indicating a lower Fe/O ratio. The higher Fe/O ratio observed by *ACE* during the rising phase is most likely due to propagation. This effect, studied by Mason et al. (2012), is a consequence of the fact that the interplanetary diffusion coefficient largely governs the initial time profiles of energetic particles. The significant difference in the charge-to-mass ratios of the O and Fe ions therefore results in increased Fe/O ratios early in the SEP event when the ratio is evaluated at a common energy/nucleon (see also Tylka et al. 2013). By integrating the intensities over the duration of the event, we obtain the energy spectra shown in Figure 6 for He, O, and Fe. The spectra are reasonably well described as a power law ($\sim E^{-\gamma}$) with indices, γ, between two and three for *STEREO-B* and close to three for *ACE*. The higher Fe/O ratio at *STEREO*-B is also evident in these plots.

The composition does have an energy dependence, however, which is illustrated in Figure 7, where the event-integrated Fe/O ratio is plotted as a function of energy for the two spacecraft. Although the ratios differ substantially at energies below a few MeV nucleon^{-1}, they have similar energy dependence, with both showing increases in the ratio with energies above

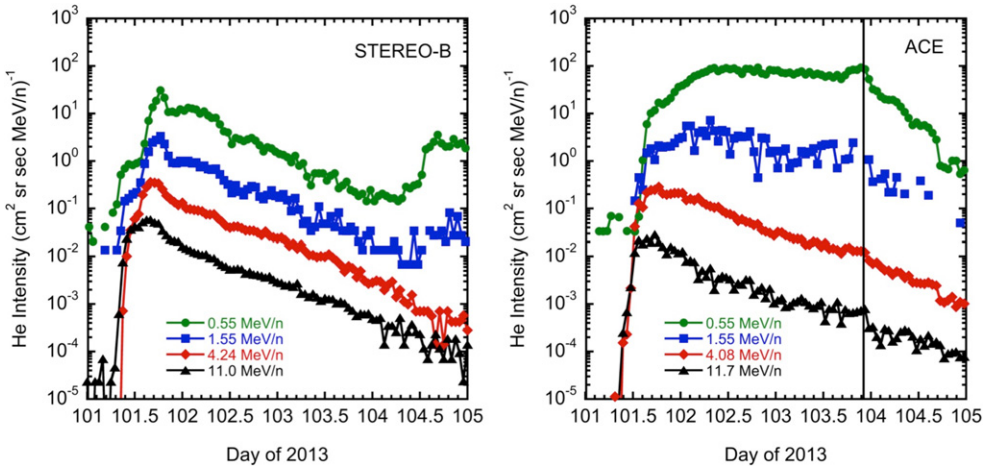

Figure 4. He intensity–time profiles at energies from 0.55 to 11 MeV nucleon^{-1} as observed by *STEREO-B* and *ACE*. The vertical line indicates the approximate shock passage time at *ACE* (no shock was observed at *STEREO-B*). The intensity increase at 104.5 at *STEREO-B* is the start of a second SEP event, which is not analyzed here.

(A color version of this figure is available in the online journal.)

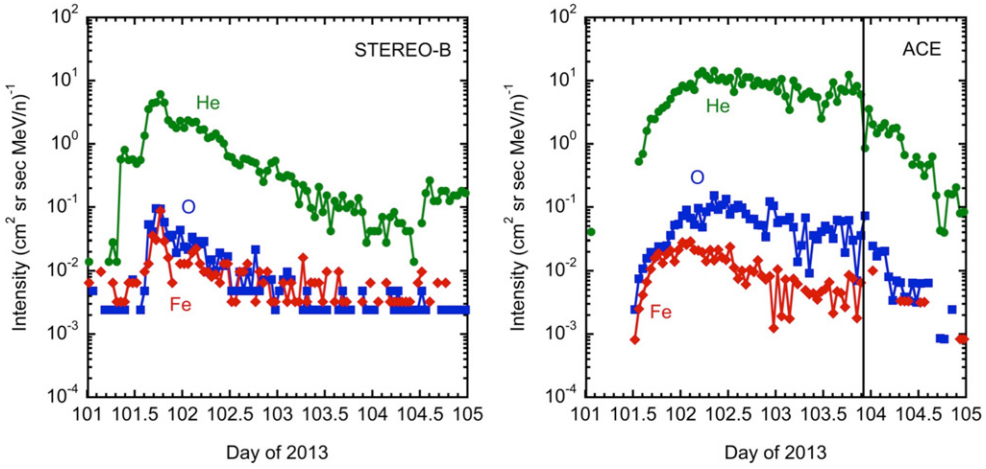

Figure 5. Intensity–time profiles for He, O, and Fe at 1.1 MeV nucleon^{-1} as observed by *STEREO* and *ACE*. The vertical line indicates the approximate shock passage time at *ACE*.

(A color version of this figure is available in the online journal.)

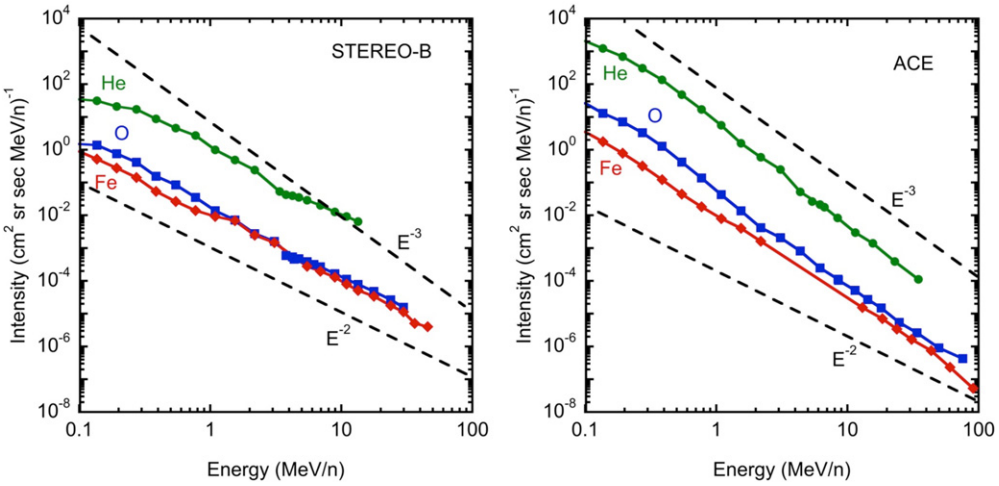

Figure 6. Event-integrated energy spectra of He, O, and Fe from *STEREO-B* (combining data from SIT and LET) and *ACE* (combining data from ULEIS and SIS). Power-law spectra with indices of 2 and 3 are shown for comparison.

(A color version of this figure is available in the online journal.)

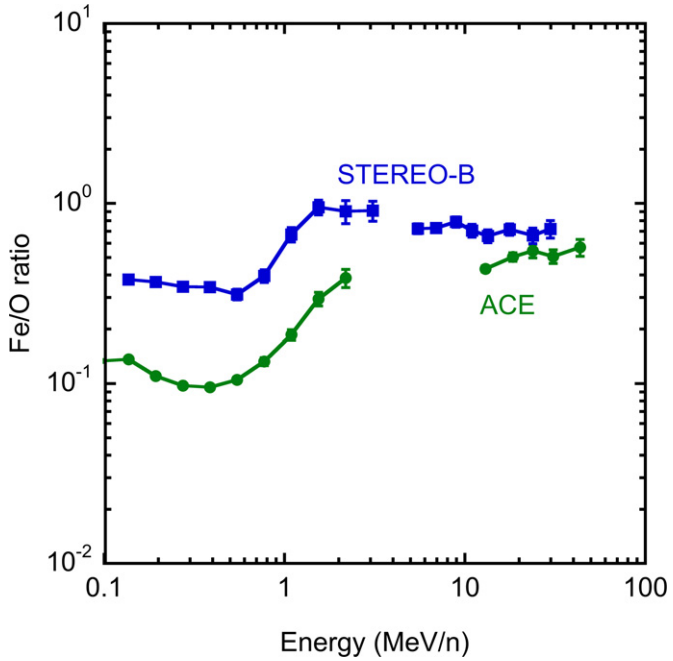

Figure 7. Fe/O abundance ratios from *STEREO-B* and *ACE* as a function of energy (integrated over the SEP event).

(A color version of this figure is available in the online journal.)

~0.5 MeV nucleon^{-1}, and at energies of ~10 MeV nucleon^{-1} reaching values substantially enhanced over the average Fe/O SEP value. For a broader comparison, the abundance ratios for 13 elements (normalized to O) obtained by integrating the spectra over 12–33 MeV nucleon^{-1} are given for *STEREO-B* and *ACE* in the left panel of Figure 8. In this energy range both spacecraft observe nearly the same composition from C to Ar; for Ca, Fe, and Ni, *STEREO-B* sees increasingly higher ratios. How this composition compares to the average gradual SEP composition is shown in the right panel of the figure, where the composition has been normalized by the Reames (1998) values. The enrichments over the average values increase with Z, particularly for ions heavier than Mg, with a pattern generally similar to that seen in the Fe-rich events observed at the start of solar cycle 23 (Cohen et al. 1999b).

The longitude dependence of the composition is illustrated in Figure 9, where He, O, and Fe fluences are plotted versus the separation between the longitude of the flaring region and that of the footpoint on the Sun of the magnetic field line passing through the location of the spacecraft (hereafter referred to as the spacecraft magnetic footpoint). The magnetic footpoints were determined by assuming a Parker spiral corresponding to the solar wind velocities observed during a few hours before the event by each spacecraft (~350 km s^{-1} for *STEREO-B* and ~380 km s^{-1} for *ACE*). As can be seen in the figure, neither spacecraft was well connected to the source region. If we assume a Gaussian distribution centered at the flare location, a width (sigma) and amplitude can be determined for each pair of points, resulting in the Gaussians shown by the solid lines. As the change in fluence from one spacecraft to the other is different for each element, the calculated sigmas are correspondingly different (e.g., it is narrower for Fe, which shows a larger change in fluence from *ACE* to *STEREO-B*).

3. DISCUSSION

The 2013 April 11 SEP event shows the largest Fe/O enrichment of any SEP event observed simultaneously from significantly different longitudes. As such it provides a unique opportunity to evaluate and compare the two distinct scenarios put forth nearly 10 years ago to explain the Fe-rich events of solar cycle 23. The fact that the Fe/O ratio increases with energy and reaches a value significantly greater than the average SEP value indicates that this is a similar event to those observed in the previous solar cycle. It also has relatively hard spectra, another characteristic of these Fe-rich events. Unfortunately, neither *ACE* nor *STEREO*-B was magnetically well connected to the solar source region, so we do not have the perfect set up to test for the direct flare contribution scenario; however one spacecraft was to the west and one to the east of the flaring region.

A previous study by Cohen et al. (2013) examined the longitude dependence of Fe/O at 10 MeV nucleon^{-1} for 12 large SEP events observed by multiple spacecraft. Only three of these events had Fe/O values at one or more of the spacecraft that were more than twice the average value. The longitudinal dependence of the Fe/O ratio for these three events (evaluated

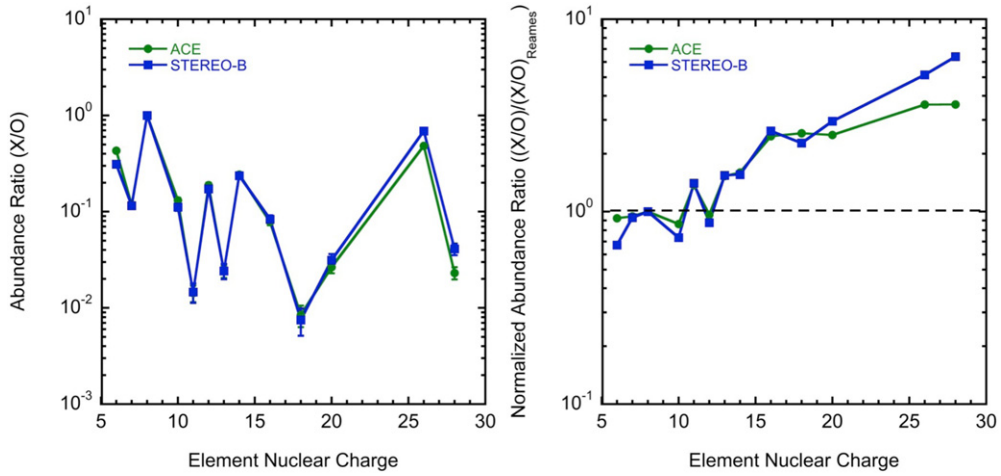

Figure 8. Left: abundance ratios at 12–33 MeV nucleon^{-1} (normalized to oxygen), integrated over the event, from *STEREO-B* and *ACE* as a function of atomic number. Right: the same abundances further normalized to average SEP abundances at 5–12 MeV nucleon^{-1} as reported by Reames (1998).

(A color version of this figure is available in the online journal.)

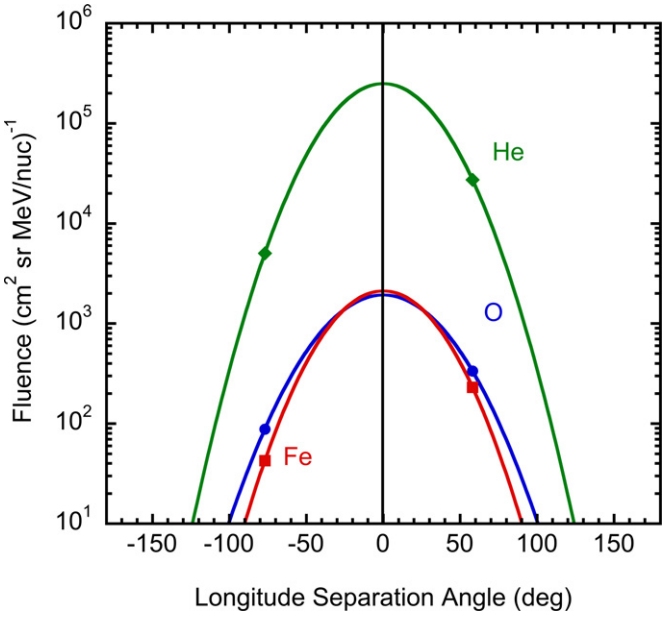

Figure 9. Event-integrated fluences (12–33 MeV nucleon^{-1}) for He (extrapolated from measurements at 12–15 MeV nucleon^{-1} assuming a power-law fit to the He spectrum shown in Figure 4), O, and Fe as a function of longitudinal separation between the flare and the spacecraft footpoints (points; *ACE* at −77° and *STEREO-B* at 58°). Assuming a Gaussian distribution centered on 0°, the corresponding calculated longitudinal dependences are shown (lines). The resulting widths are 28°, 31°, and 28° for He, O, and Fe, respectively.

(A color version of this figure is available in the online journal.)

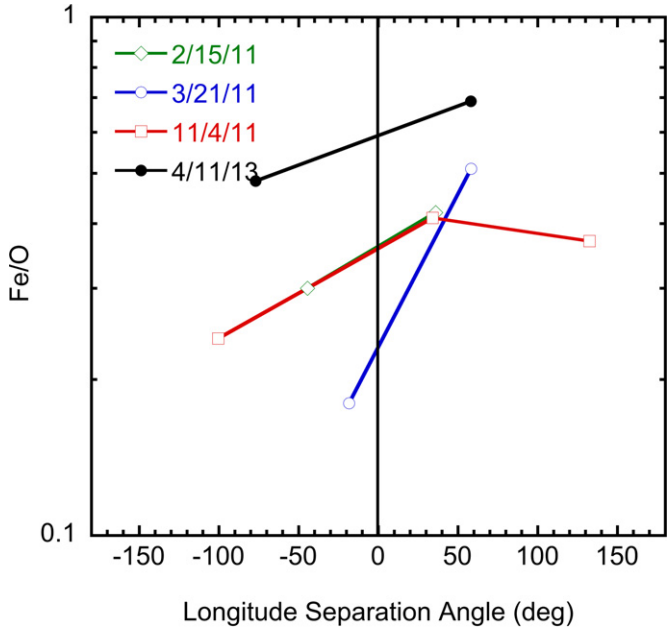

Figure 10. Fe/O abundance as a function of the longitudinal separation between the spacecraft magnetic footpoint (assuming a Parker spiral) and the location of the flare for the 2013 April 11 event (at 12–33 MeV nucleon^{-1}) and three other cycle 24 events with Fe/O abundances enhanced by ⩾2 (at 10 MeV nucleon^{-1}; from Cohen et al. 2013). Only the 2011 November 4 event had measureable Fe and O abundances at all three spacecraft (*STEREO-B*, *ACE*, and *STEREO-A*).

(A color version of this figure is available in the online journal.)

at 10 MeV nucleon^{-1}), as well as for the 2013 April 11 event (evaluated at 12–33 MeV nucleon^{-1}), is shown in Figure 10. The 2013 April 11 event stands out as being significantly more Fe-rich than the other events. Although it is difficult to draw firm conclusions from so few events (and the fact that there were no measurements made within 15° of the longitude connected to the flare site for any of the events), it is not clear that the longitudinal distribution peaked at the flare connection longitude (e.g., 0° in the plot). In particular, the 2011 March 21 event exhibits a higher Fe/O ratio for the less well-connected observer and the three measurements made in the 2011 November 4 event are inconsistent with a Gaussian centered at the flare location. It is possible that the longitudinal dependence is neither a Gaussian nor symmetric about the flare site (e.g., see Mewaldt et al. 2005; Lario et al. 2013), however, it is not possible to determine this from the current heavy-ion data.

The longitudinal dependences of the fluences shown in Figure 9 are potentially consistent with the direct flare contribution, in that the Fe fluences correspond to a narrower distribution than that of O. This could be due to more Fe (relative to He or O) being produced close to the flare location, which results in a very high Fe/O ratio at small longitudinal separations. If we assume Gaussian distributions centered at 0° separation, the corresponding interpolated Fe/O ratio at the connection longitude of the flare is 1.1, which is higher than any of the Fe/O ratios observed in the Fe-rich SEP events of cycle 23 (Cane et al. 2006;

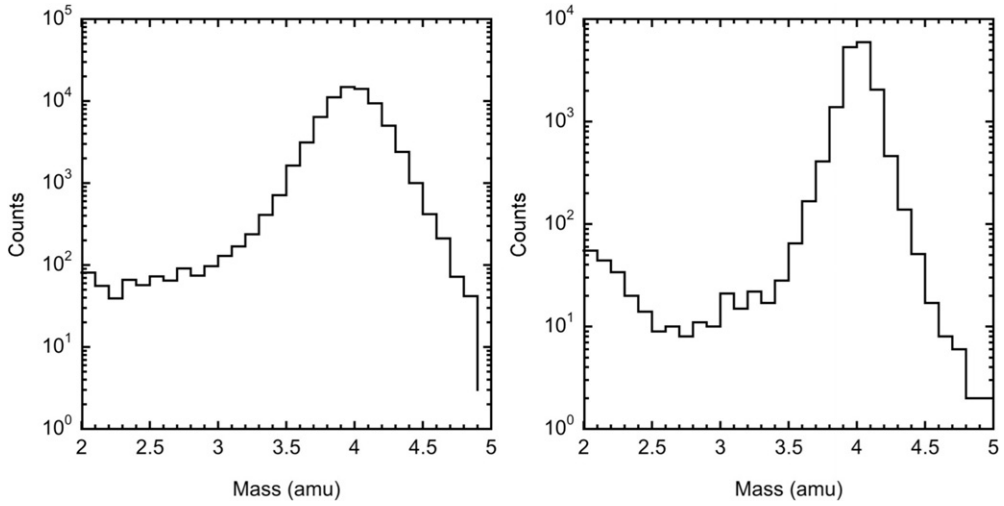

Figure 11. He mass histograms integrated over the 2013 April 11 event from *STEREO-B*/LET at 4.3–8.0 MeV nucleon^{-1} (left) and *ACE*/ULEIS at 0.5–2.0 MeV nucleon^{-1} (right). Derived upper limits are 4% and 0.07% from *STEREO-B*/LET and *ACE*/ULEIS, respectively.

Cohen et al. 2008), but typical of impulsive events (Reames 1998). However, the derived distributions for He, O, and Fe are significantly narrower (widths of 28°, 31°, and 28°, respectively) than those obtained for H, He, O, and Fe in previous studies (e.g., Lario et al. 2006, 2013; Mewaldt et al. 2013; Cohen et al. 2014) where all elements exhibited widths of 40°–50°. We could have assumed a nominal and uniform width of ∼45° for all elements and calculated the amplitude and center of the Gaussians consistent with the observed fluences. However, as the fluences at *STEREO*-B relative to *ACE* are not the same for He, O, or Fe, this would have resulted in different locations for the Gaussian centers, a characteristic not expected from any of the suggested scenarios.

The work of Lario et al. (2006, 2013) shows that the longitudinal distributions of proton peak intensities are best fit with a Gaussian that is not centered at 0° separation between the flare and the magnetic footpoint of the observing spacecraft: $j = j_0 \exp[-(\phi-\phi_0)^2/2\sigma^2]$, where ϕ_0 is the offset, ϕ is the separation between the flare and the magnetic footpoint of the spacecraft, and σ is the width of the distribution. They find that on average an offset, ϕ_0, of $-12° \pm 3°$ best matches their data (Lario et al. 2013). Using a similar offset to fit the observations of 2013 April 11 results in a distribution center that is closer to the *ACE* points than to the *STEREO-B* points, which makes it impossible to use Gaussian fits (as the *ACE* fluences are lower than those of *STEREO-B*). Moving the center of the distribution closer to *ACE* (i.e., to the left in Figure 9; westward from the flare location on the Sun) requires narrower Gaussians to fit the observations and increases the interpolated Fe/O ratio at the distribution center. The largest possible (integer) offset in the same direction as that found by Lario et al. that still allows Gaussian fits is −9° and yields widths of 6°, 7°, and 6° for He, O, and Fe, respectively, and an interpolated Fe/O ratio at the center that is not physically possible. To obtain sigmas similar to those observed by Mewaldt et al. (2013) and Cohen et al. (2014), the center of the Gaussian distribution would need to be offset in the opposite direction (i.e., toward *STEREO-B*; to the right in Figure 9; eastward from the flare location on the Sun) to that determined by Lario et al. by 10°–15°.

The differing widths for each element (Figure 9) and the higher Fe/O ratio closer to the flare location (Figure 10) are both potentially inconsistent with the remnant flare suprathermal theory, which generally predicts no longitudinal dependence to the composition. However, the likelihood of a shock being quasi-perpendicular is higher along the flanks of a CME (assuming a nominal Parker spiral configuration to the interplanetary magnetic field), thus one might expect higher Fe/O ratios in those locations. This would be consistent with the observations of high Fe/O ratios at *ACE* and *STEREO-B* in the 2013 April 11 event, as both spacecraft magnetic footpoints were far from the flare location and thus more likely to intercept the flanks of the outgoing CME-driven shock. The differing Fe/O enhancements observed at the two spacecraft would then require a longitudinal dependence to the flare suprathermal composition or density, or significant differences in the acceleration conditions (e.g., the injection threshold energy or orientation of the shock) at the two locations.

Another characteristic of the Fe-rich SEP events of cycle 23 was the observed enhancement of ^{3}He/^{4}He. Unfortunately, the mass resolution of the LET instrument on *STEREO-B* is not as high as that of the ULEIS or SIS sensors on *ACE*, making it difficult to determine ^{3}He/^{4}He ratios below 4% in large SEP events (due to the spillover from the ^{4}He peak). The 2013 April 11 He mass histograms are shown in Figure 11; there is no discernable ^{3}He peak in either the *STEREO-B* or *ACE* observations. Using data from both ULEIS (right panel, Figure 11) and SIS (not shown in Figure 11, see Figure 12), we derive upper limits of 0.07% and 1% for the *ACE* ^{3}He/^{4}He ratio at 0.5–2 and 6.5–11.3 MeV nucleon^{-1}, respectively, whereas the upper limit from *STEREO-B*/LET (left panel, Figure 11) is 4% (see also Table 1). For comparison, the ULEIS and SIS He mass histograms are shown in Figure 12 for two cycle 23, Fe-rich events along with the 2013 April 11 event. Of the first four cycle 23, Fe-rich events, ULEIS measurements are available for 1997 November 4 and 1998 May 6. In both cases a ^{3}He peak is seen, corresponding to ^{3}He/^{4}He ratios of 0.165% and 0.532%, respectively (Desai et al. 2006). The SIS observations made in the 1998 May 2 event are shown in the right panel along with the 1998 May 6 event. The 1998 May 2 event was selected for comparison, as it was the Fe-rich event with the lowest ^{3}He/^{4}He ratio measured by SIS, corresponding to an upper limit of 0.2% (at 8–14 MeV nucleon^{-1}; Cohen et al. 1999b; Table 1). The reported ^{3}He/^{4}He ratio for the 1998 May 6 at this energy range was 4%. Figure 12 illustrates that at 6.5–11.3 MeV nucleon^{-1} the 2013 April 11 event has potentially even less ^{3}He than that seen in the 1998 May 2 event. The lack of a ^{3}He enhancement

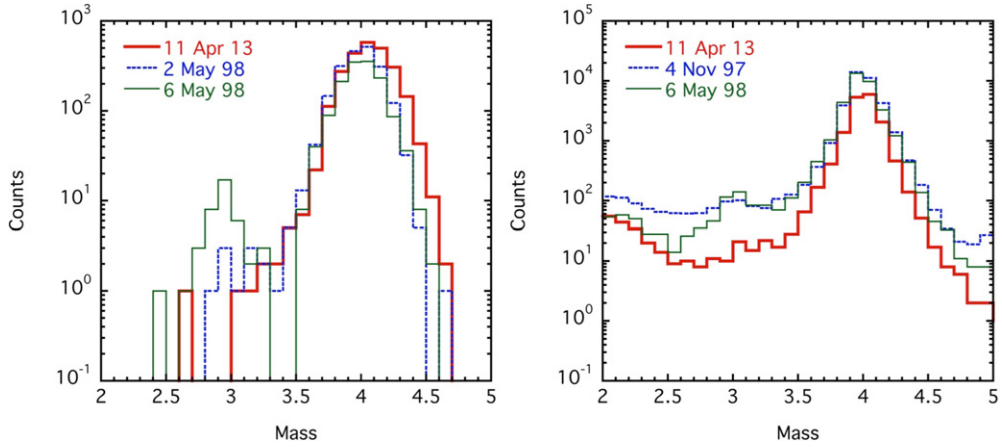

Figure 12. He mass histograms from *ACE*/SIS at 6.5–11.3 MeV nucleon^{-1} (for ^{4}He and slightly higher for ^{3}He) (left) and *ACE*/ULEIS at 0.5–2.0 MeV nucleon^{-1} (right) for the April 11 event as compared to two Fe-rich SEP events in cycle 23. ULEIS only observed the 1997 November 4 and 1998 May 6 events; the 1998 May 2 event observed by SIS had the lowest ^{3}He/^{4}He abundance of the measured Fe-rich events in cycle 23, whereas 1998 May 6 had the highest.

(A color version of this figure is available in the online journal.)

Table 1
He/^{4}He Values

Event date	*ACE*/ULEIS 0.5–2.0 MeV nucleon^{-1}	*ACE*/SIS 8–14 MeV nucleon^{-1}	*STEREO-B*/LET 4.3–8.0 MeV nucleon^{-1}
1997 Nov 4	0.165%	0.7 %	
1998 May 2		<0.2%	
1998 May 6	0.534%	4%	
2013 Apr 11	<0.07%	<1%[a]	<4%

Note. [a] Measured at 6.5–11.0 MeV nucleon^{-1}.

observed by *ACE* in the 2013 April 11 event is rather surprising given the high Fe/O ratio (and other characteristics similar to the cycle 23 Fe-rich events). If the ^{3}He/^{4}He ratio exhibited the same longitudinal dependence as the Fe/O ratio, we would expect a *STEREO-B* ^{3}He/^{4}He ratio of <1.5% at SIS energies, or <0.11% at ULEIS energies; both of which are consistent with the LET observations. These upper limits are still below most of the values observed in the Fe-rich events of cycle 23. However, the magnitude of the enhancements in Fe/O and ^{3}He/^{4}He are not clearly correlated for the cycle 23 Fe-rich events, so there is no a priori reason to expect similar longitudinal dependences for the two abundance ratios. Further, if the longitudinal spread is largely a result of processes dependent on the charge-to-mass (Q/M) ratio of an element, the spreads of the Fe/O and ^{3}He/^{4}He ratios would be different, as $(Q/M)_{\rm Fe}/(Q/M)_{\rm O}$ is very different than $(Q/M)_{\rm 3He}/(Q/M)_{\rm 4He}$ for typical SEP values of Q.

In considering the implications of the ^{3}He/^{4}He results for the Cane et al. (2003) and Tylka et al. (2005) scenarios, we examine two possibilities for the ^{3}He/^{4}He ratio at *STEREO-B*: (1) it is enhanced, possibly as high as 4%, or (2) it is similar to the upper limits derived from the *ACE* observations. Case (1) would indicate that the longitudinal dependence of ^{3}He/^{4}He is distinctly different than that of Fe/O (at least at energies >10 MeV nucleon^{-1} where the Fe/O ratios differ by only 44% between the two spacecraft), with the ^{3}He/^{4}He having a narrower spread in longitude. Assuming a ratio at *STEREO-B* of 4% and a Gaussian distribution centered at the flare location, the corresponding ^{3}He/^{4}He ratio interpolated to the flare location would be 26%, which is many times what has been previously measured in large Fe-rich SEP events, even from well-connected observers. Interpreted according to the remnant flare material scenario, case (1) would either indicate a seed population with a non-uniform composition or density in longitude and/or substantially different efficiencies of accelerating remnant ^{3}He, relative to ^{4}He, at locations well connected to *STEREO-B* and *ACE*. The former is perhaps not unreasonable as there would likely be different solar sources (e.g., prior flares) for the remnant material at the two locations.

Case (2) would be potentially problematic for both the direct flare contribution and remnant flare material scenarios, as in both cases ^{3}He/^{4}He enhancements are expected to result from the same conditions that create the enhancements in Fe/O (i.e., contribution of flare material). Although surprising, the low ^{3}He/^{4}He observed by *ACE* is not without precedent. In addition to the 1998 May 2 event measured by SIS, the 2006 December 13 Fe-rich event also exhibited low values of ^{3}He/^{4}He (Cohen et al. 2008). Alternatively, if the lack of enhanced ^{3}He/^{4}He is evidence that flare material (directly or through the seed population) is not generating the observed high Fe/O ratios, then another mechanism must be found. One possibility is the effect of interplanetary transport, such as that described and modeled by Mason et al. (2006, 2012). The application of this model, tuned to best match the observations of the 2013 April 11 event, is beyond the scope of this paper. There is some indication at lower energies of a time dependence to the *STEREO-B* Fe/O ratio (decreasing with time) for the first few hours of the event, similar to the 2005 January event studied in the Mason et al. (2012) paper, however, the model will not explain the sustained enhancement of Fe/O observed throughout the event.

Further complicating the interpretation of the observed and expected ^{3}He/^{4}He ratios, is the recent observation by Wiedenbeck et al. (2013) of wide longitudinal spreads of ^{3}He-rich SEP events. The authors identified several ^{3}He-rich, impulsive SEP events that were measured by the *ACE* and *STEREO*

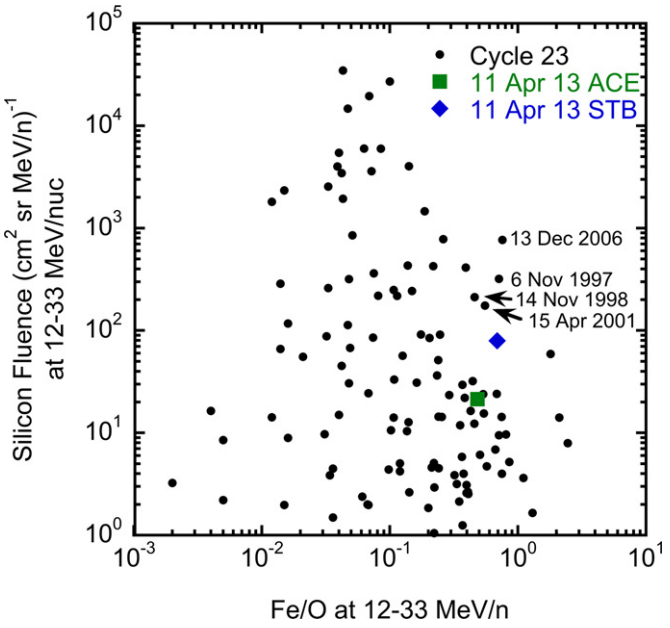

Figure 13. Fluence of Si (event-integrated) versus the Fe/O ratio at 12–30 MeV nucleon^{-1} for the cycle 23 SEP events measured by *ACE*/SIS. Measurements from *ACE* and *STEREO-B* for the 2013 April 11 event are indicated individually by the solid symbols. (All the events with Fe/O > 1 are identified as impulsive SEP events, see, e.g., Wiedenbeck et al. 2003) The 1997 November 6, 1998 November 14, 2001 April 15, and 2006 December 13 events are indicated by labels next to the points.

(A color version of this figure is available in the online journal.)

spacecraft when the separation of the spacecraft was >60°. This is in contrast to the generally accepted expectation that a spacecraft must be within ∼20° of the longitude of the magnetic connection to the flaring region in order to observe the enhanced ^{3}He/^{4}He ratio typical of flare-accelerated material (e.g., Reames 1999). Using observations made by both *STEREO*s and *ACE* during the 2010 February 7 SEP event, the authors derived a Gaussian width of 48° for the longitudinal dependence of the ^{3}He fluence. This is comparable to the widths determined for protons and heavy ions in many SEP events (Lario et al. 2013, 2006; Mewaldt et al. 2013) and, if typical, would weaken the longitudinal dependence of the composition as predicted by the direct flare contribution scenario.

Figure 13 shows how the 2013 April 11 event compares to cycle 23 events. The event-integrated fluence of Si (at 12–33 MeV nucleon^{-1}) is plotted versus the event-integrated Fe/O ratio (at 12–33 MeV nucleon^{-1}) for all events with Si fluences >1 (cm^2 Sr MeV nucleon $^{-1}$) $^{-1}$ (see also Mewaldt et al. 2006). The 2013 April 11 values from *ACE* and *STEREO-B* are given by the large solid square and diamond, respectively. The *STEREO-B* measurement is consistent with the pattern of Fe-rich SEP events being moderate in size (N.B.: the five events with Fe/O > 1 have all been identified as ^{3}He-rich/impulsive SEP events by Wiedenbeck et al. 2003). Four cycle 23 events with either similar Fe/O ratios and/or similar Si fluences to that measured by *STEREO-B* are indicated in Figure 13: 1997 November 6 (Fe/O = 0.71), 1998 November 14 (Fe/O = 0.55), 2001 April 15 (Fe/O = 0.46), and 2006 December 13 (Fe/O = 0.76). All these events have been previously discussed for their compositional properties (Cohen et al. 1999a, 1999b, 2008; Tylka et al. 2002). The 1997 November 6 and 2006 December 13 events had longitudinal separations between the flare and the spacecraft magnetic footpoints of −6° and 6°, respectively, while the other two events had larger separations of 30° and 25° (1998 November 14 and 2001 April 15, respectively), which were all substantially smaller than the 74° for *STEREO*-B in the 2013 April 11 event. With the exception of the 2006 December 13 event, all the events had observed enhancements in ^{3}He/^{4}He. Unfortunately, three of the events occurred well before the *STEREO* launch (2006 October) and the 2006 December 13 event happened while both *STEREO* spacecraft were relatively close to Earth, thus, no information is available for the longitudinal dependence of the composition in these events.

4. SUMMARY

The 2013 April 11 SEP event was the first large SEP event in solar cycle 24 with a ⩾10 MeV nucleon^{-1} Fe/O abundance more than five times the average Fe/O abundance found in gradual SEP events. As the composition of this event was measured by both the *STEREO-B* and *ACE* spacecraft, it provides an opportunity to examine the longitudinal dependence of the Fe/O ratio, as well as potentially test scenarios put forth to explain similar Fe-rich SEP events from cycle 23. Although the magnetic footpoints of the two spacecraft were similarly separated from the flare, but in opposite directions, there are significant differences in the Fe/O abundances, with *STEREO-B* (with the flare located west of the footpoint) observing a Fe/O ratio higher by 44% than that seen by *ACE* (with the flare located east of the spacecraft footpoint). Contrary to most Fe-rich events of cycle 23, there was no significant enhancement in the ^{3}He/^{4}He abundance at *ACE*. It is not possible to put a strong upper limit on this ratio at *STEREO-B*. For elements C through Ar, the abundances relative to O are very similar at both spacecraft, with elements heavier than Mg showing enhancements of factors of ∼2–5.

The assumption of a Gaussian distribution centered at the flare location produces widths (sigmas) that are significantly narrower than those seen in previous events in cycles 23 and 24. With measurements at only two locations it is not possible to determine whether the longitudinal distribution is uniquely described by a Gaussian, but it is clear that the standard offset of the Gaussian center from the flare location typically used by Lario et al. (2006, 2013) is not consistent with the data. Additionally, observations of other SEP events with moderate Fe enhancements suggest longitudinal distributions that are either non-Gaussian or asymmetric about the flare location.

The longitude dependence observed in the Fe/O ratio is compatible with the direct flare contribution scenario suggested by Cane et al. (2003) in that the observer closer to the flare observes the higher Fe/O ratio, although neither observer is well connected to the flare in this event. A longitude dependence to the suprathermal seed population or significant differences in the acceleration conditions on the opposing sides of the CME-driven shock would be required for the remnant flare material theory of Tylka et al. (2005) to be consistent with the observations. The lack of a ^{3}He/^{4}He enhancement at *ACE* is potentially inconsistent with both scenarios, unless the flare or flare suprathermal ^{3}He/^{4}He ratio near the Sun has a significantly narrower longitudinal spread than that of the Fe/O ratio. The rise-phase enhancement of the Fe/O ratio at *STEREO-B* may be the result of interplanetary transport effects, however, it is unclear how this would generate the sustained high Fe/O ratios seen throughout the event at *ACE* and *STEREO-B*. Detailed examination and modeling of the *STEREO-B* and *ACE* abundances as a function of time throughout the event would be required to investigate this possibility in the future.

This work was supported by NASA at Caltech and JPL under subcontract SA2715-26309 from UC Berkeley under NASA contract NAS5-03131T, and by NASA grants NNX11A075G and NNX13AH66G. It was also supported by the NSF under the grant 1156004. Work at APL was supported by NASA grants NNX13AR20G and 44A-1091698, as well as NSF SHINE grant 1156138 and UC Berkeley subcontract SA4889-26309. We thank the NASA CDAW Data Center and the Catholic University of America and ESA's CACTus project for their CME catalogs. We also thank the Michigan State University National Superconducting Cyclotron Lab for accelerator time and staff assistance in calibrating the response of the *ACE*/SIS and *STEREO*/LET sensors to energetic ions and in testing the related onboard analysis processes.

REFERENCES

Cane, H. V., Mewaldt, R. A., Cohen, C. M. S., & von Rosenvinge, T. T. 2006, JGR, 111, A06590
Cane, H. V., Reames, D. V., & von Rosenvinge, T. T. 1988, JGR, 93, 9555
Cane, H. V., von Rosenvinge, T. T., Cohen, C. M. S., & Mewaldt, R. A. 2003, GeoRL, 30, 8017
Cohen, C. M. S., Cummings, A. C., Leske, R. A., et al. 1999a, GeoRL, 26, 149
Cohen, C. M. S., Mason, G. M., Mewaldt, R. A., & von Rosenvinge, T. T. 2013, in AIP Conf. Proc. 1539, SOLAR WIND 13: Proceedings of the Thirteenth International Solar Wind Conference, ed. G. Zank, J. Borovsky, R. Bruno et al. (Melville, NY: AIP), 151
Cohen, C. M. S., Mason, G. M., Wiedenbeck, M. E., et al. 2012, in AIP Conf. Proc. 1436, Physics of the Heliosphere: A 10 Year Retrospective: Proceedings of the 10th International Astrophysics Conference, ed. J. Heerikhuisen, G. Li, N. Pogorelev, & G. Zank (Melville, NY: AIP), 103
Cohen, C. M. S., Mewaldt, R. A., Leske, R. A., et al. 1999b, GeoRL, 26, 2697
Cohen, C. M. S., Mewaldt, R. A., & Mason, G. M. 2014, in AIP Conf. Proc., in press
Cohen, C. M. S., et al. 2008, in AIP Conf. Proc. 1039, Particle Acceleration and Transport in the Heliosphere and Beyond, ed. G. Li, Q. Hu, O. Verkhoglyadova et al. (Melville, NY: AIP), 118
Desai, M. I., Mason, G. M., Gold, R. E., et al. 2006, ApJ, 649, 470
Lario, D., Kallenrode, M.-B., Decker, R. B., et al. 2006, ApJ, 653, 1531
Lario, D., Aran, A., Gómez-Herrero, R., et al. 2013, ApJ, 767, 41
Li, G., Zank, G. P., & Rice, W. K. M. 2005, JGR, 110, A06104
Mason, G. M., Cohen, C. M. S., Cummings, A. C., et al. 1999, GeoRL, 26, 141
Mason, G. M., Desai, M. I., Cohen, C. M. S., et al. 2006, ApJL, 647, L65
Mason, G. M., Gold, R. E., Krimigis, S. M., et al. 1998, SSRv, 86, 409
Mason, G. M., Korth, A., Walpole, P. H., et al. 2008, SSRv, 136, 257
Mason, G. M., Li, G., Cohen, C. M. S., et al. 2012, ApJ, 761, 104
Mewaldt, R. A., Cohen, C. M. S., Cook, W. R., et al. 2008, SSRv, 136, 285
Mewaldt, R. A., Cohen, C. M. S., Mason, G. M., et al. 2005, in Proc. Solar Wind 11-*SOHO* 16, ed. B. Fleck, T. H. Zurbuchen, & H. Lacoste (ESA SP-592; Noordwijk: ESA), 67
Mewaldt, R. A., Cohen, C. M. S., Mason, G. M., et al. 2006, GMS, 165, 115
Mewaldt, R. A., Cohen, C. M. S., Mason, G. M., et al. 2013, in AIP Conf. Proc. 1539, SOLAR WIND 13: Proceedings of the Thirteenth International Solar Wind Conference, ed. G. Zank, J. Borovsky, R. Bruno et al. (Melville, NY: AIP), 116
Reames, D. V. 1998, SSRv, 85, 327
Reames, D. V. 1999, SSRv, 90, 413
Richardson, I. G., von Rosenvinge, T. T., Crane, H. V., et al. 2014, SoPh, 289, 3059
Stone, E. C., Cohen, C. M. S., Cook, W. R., et al. 1998, SSRv, 86, 357
Tylka, A. J., Boberg, P. R., Cohen, C. M. S., et al. 2002, ApJL, 581, L119
Tylka, A. J., Cohen, C. M. S., Dietrich, W. F., et al. 2005, ApJ, 625, 474
Tylka, A. J., & Lee, M. A. 2006, ApJ, 646, 1319
Tylka, A. J., Malandraki, O. E., Dorrian, G., et al. 2013, SoPh, 285, 251
Wiedenbeck, M. E., Leske, R. A., Cohen, C. M. S., et al. 2003, in Proc. of the 28th ICRC, ed. T. Kajita, Y. Asaoka, A. Kawachi, Y. Matsubara, & M. Sasaki (Tokyo: Universal Academy Press), 3245
Wiedenbeck, M. E., Mason, G. M., Cohen, C. M. S., et al. 2013, ApJ, 762, 54